

Messinian astrochronology of the Melilla Basin: Stepwise restriction of the Mediterranean–Atlantic connection through Morocco

E. van Assen^a, K.F. Kuiper^{a,b,*}, N. Barhoun^c, W. Krijgsman^a, F.J. Sierro^d

^a Paleomagnetic Laboratory “Fort Hoofddijk”, Utrecht University, Budapestlaan 17, 3584 CD Utrecht, The Netherlands

^b Department of Isotope Geochemistry, Faculty of Earth and Life Sciences, Vrije Universiteit, De Boelelaan 1085, 1081 HV Amsterdam, The Netherlands

^c Department of Geology, Faculty of Science Ben M'sik, University of Casablanca, Morocco

^d Department of Geology, University of Salamanca, 37008 Salamanca, Spain

Received 17 January 2003; accepted 7 March 2006

Abstract

The Melilla Basin (NE Morocco) formed the easternmost part of the Rifian Corridor, which was an important Mediterranean–Atlantic gateway during the Late Miocene. The sedimentary infill of the basin consists of a shallow marine, precession-related cyclic marl–diatomite succession, laterally grading into a marginal carbonate complex. Three bio-sedimentary events have been recorded within the marl succession: 1) onset of diatomite deposition, 2) major change in foraminiferal assemblages, and 3) transition to *Halimeda*-rich carbonates and *Porites* coral reef build-ups. Recent ⁴⁰Ar/³⁹Ar dating has provided a good age control for the Melilla carbonate sequences, but a high-resolution astronomical time frame is necessary to solve the climatic signature of the basin sediments.

This study focuses on the shallow marine marl succession of the Melilla Basin. Integrated magneto-, cyclo- and biostratigraphy allowed a detailed correlation to the astronomical target curve, resulting in a high-resolution time frame for the Late Miocene evolution of the basin. Comparison of the Melilla data with previous results from other Moroccan and Mediterranean basins indicates that the input of Atlantic waters through the Rifian Corridor became restricted after 6.84 Ma, and was minimized by 6.58 Ma. In the final period (6.58–5.96 Ma) towards the Messinian Salinity Crisis, the Melilla Basin can be considered as a marginal basin of the Mediterranean.

The astronomical time frame for the marl sequences of the Melilla Basin moreover enables a direct comparison between the independent isotopic and astrochronological dating techniques, as astronomical ages have also been assigned to intercalated volcanic tuffs for which ⁴⁰Ar/³⁹Ar ages were previously determined. We conclude that the isotopic ages are systematically younger than their astronomical equivalents.

© 2006 Elsevier B.V. All rights reserved.

Keywords: Mediterranean; Messinian; Morocco; Astronomical cyclicity; Diatomites

1. Introduction

During the Late Miocene, the Mediterranean was connected to the Atlantic Ocean through at least two marine gateways: the Betic and Rifian Corridors (e.g.

* Corresponding author. Tel.: +31 30 2535418; fax: +31 30 2531677.
E-mail address: kkuiper@geo.uu.nl (K.F. Kuiper).

Benson et al., 1991). The evolution of these corridors is of major importance to our understanding of the Late Neogene isolation of the Mediterranean Sea, which resulted in the Messinian Salinity Crisis. The recently developed Astronomical Time Scale (ATS) for the Messinian of the Mediterranean Realm (Hilgen et al., 1995; Krijgsman et al., 1999a) can now be used for detailed analysis of the paleogeographic evolution of these Neogene gateways.

The Melilla Basin in northeastern Morocco forms the easternmost part of the Rifian Corridor (Fig. 1). The sedimentary succession of this basin consists of an Upper Miocene carbonate platform, grading laterally into basal marine clays, marls and laminites, which display

repetitive lithological alternations (Choubert et al., 1966; Gaudant et al., 1994; Saint Martin and Cornée, 1996). The intercalation of volcano-clastic levels provides a correlation tool between the basinal sequences and the carbonate-platform (Cunningham et al., 1994; Cunningham et al., 1997; Roger et al., 2000). Isotopic dating of these volcanic ashes has provided a scenario in three stages of the pre-evaporitic Messinian basin-evolution (Roger et al., 2000; Münch et al., 2001); 1) the onset of a prograding bioclastic carbonate unit, coeval with the onset of diatomaceous marl deposition, 2) a transition to warm-water conditions, evidenced by the start of warm-water diatomites and prograding *Porites* coral reefs, and 3) the termination of the prograding carbonate complex.

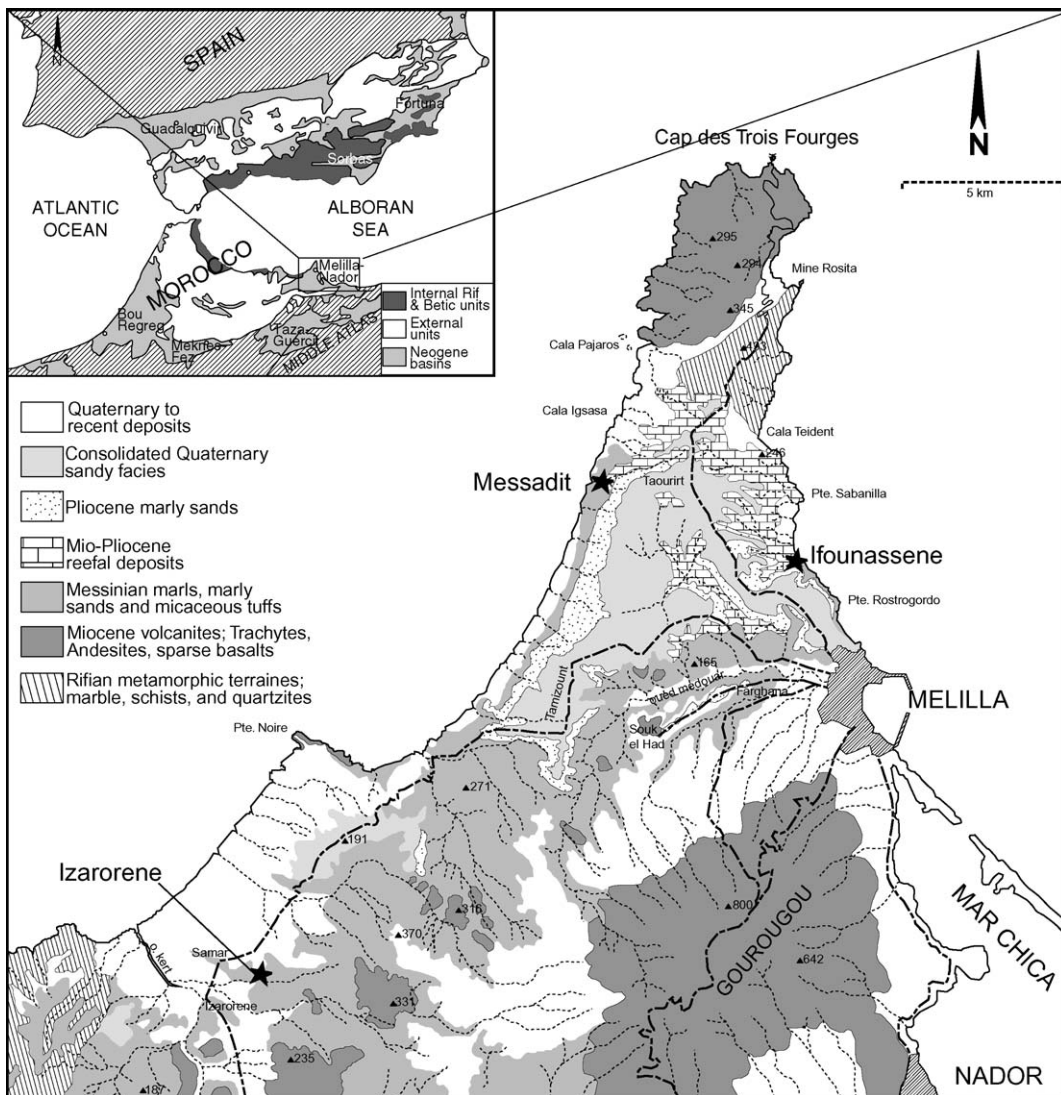


Fig. 1. Geographic location of the sampled sections in the Melilla Basin, Northeast Morocco. The main geologic units included in the figure are based on the work of Choubert et al. (1966).

Our current study focuses on the astronomical tuning of the cyclically developed marls of the Melilla Basin. This paper presents a detailed integrated bio-, magneto- and cyclostratigraphy of the basinal sedimentary sequence, which enables a direct bed-to-bed correlation to the Late Miocene framework of the Mediterranean (Hilgen et al., 1995; Sierro et al., 2001; Krijgsman et al., 2001, 2002) and open ocean records (Hodell et al., 2001). Additionally, astronomical ages are derived for the intercalated volcanic ashes, which allow a direct comparison with isotopic ($^{40}\text{Ar}/^{39}\text{Ar}$) ages obtained from the carbonate platform (Cunningham et al., 1994, 1997; Roger et al., 2000; Münch et al., 2001).

2. Geological setting

The Melilla Basin is located along the northeastern coast of Morocco and is named after the Spanish enclave located on the peninsula of Cap de Trois Fourges (Fig. 2). The basin extends from the peninsula towards Algeria in the east and the Rif Mountains near Tamsaman in the west (Guillemin and Houzay, 1982), and is bordered to the south by the remnants of the folded structures of the metamorphic Rif foreland.

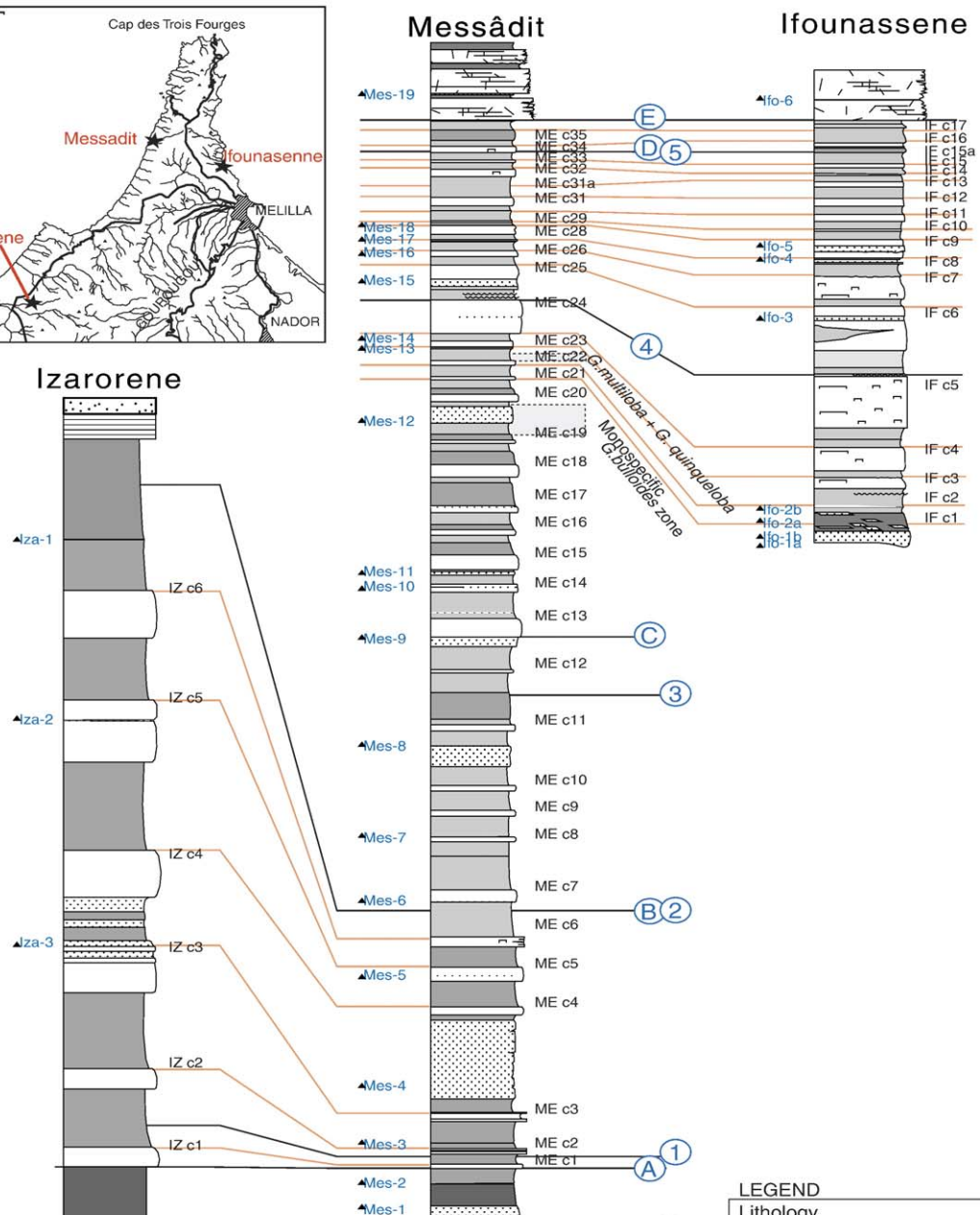
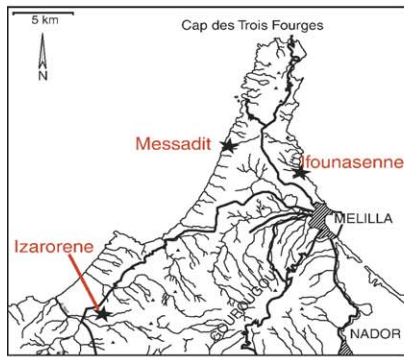
The basin formed after the main orogenic movements of the Rif during the Middle Miocene (Choubert et al., 1966; Guillemin and Houzay, 1982). An early extensional phase commenced during the Serravallian, and resulted in the deposition of a molassic “clastic wedge” accompanied by rhyolitic volcanism (El Bakkali et al., 1998). This phase was followed by a N–S directed compression, which resulted in uplift of the Paleozoic metamorphic core complex of the Melilla peninsula. A transgressive conglomerate of an assumed Late Tortonian age (Choubert et al., 1966; Guillemin and Houzay, 1982) indicates the final Miocene, basin-forming extension, which provided the accommodation space for basinal marl deposition and the formation of a marginal carbonate platform. This phase ended with a lagoonal to lacustrine regressive sequence (Arias et al., 1976; Barbieri et al., 1976; Saint Martin et al., 1991). Frequent coeval volcanism of the acidic Trois Fourges and alkaline Gourougou volcanoes resulted in the deposition of numerous ashes within these sediments and the development of seismites (El Bakkali et al., 1998). Deposition of a transgressive sandy facies, supposedly of Pliocene age (Choubert et al., 1966; Guillemin and Houzay, 1982) and unconformably overlying the open marine sequence is followed by a final compressional phase, uplifting the basin to its present altitude above sea level.

The Neogene sediments are best exposed on the Melilla peninsula. South of the Cap de Trois Fourges, a well-developed carbonate complex is formed, laterally grading into a basinal, silty to clayey marl sequence, including laminites and diatomites (Saint Martin and Cornée, 1996; Münch et al., 2001). The end of the basinal marl deposition is marked by a final diatomite bloom, which is generally associated to upwelling (Saint Martin et al., 1991; Roger et al., 2000), followed by deposition of a *Halimeda*-algae packstone. This *Halimeda*-unit, indicating the final stage of the prograding bioclastic carbonate unit (Cunningham et al., 1994), can be traced towards the carbonate complex. The latter is overlain by a topography-draping marine-to-continental transitional sequence composed of grainstones, reefs and stromatolites, referred to as the Terminal Carbonate Complex (TCC of Cunningham et al., 1994).

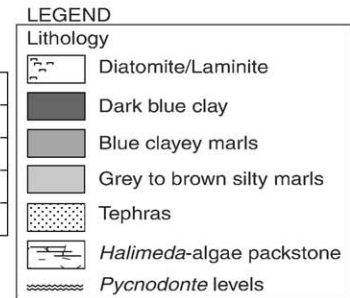
Previous works mainly concerned the carbonate platform, which displays a reef-geometry characteristic for the Alboran Basin (Saint Martin and Rouchy, 1986; Cornée et al., 1996; Saint Martin and Cornée, 1996). The timing of reef development is based on paleomagnetic analysis and isotopic ($^{40}\text{Ar}/^{39}\text{Ar}$) dating of intercalated ashes within the carbonate complex and transition zone (Cunningham et al., 1994; Cunningham et al., 1997; Roger et al., 2000). These studies have resulted in the first age-constraints of three major bio-sedimentary phases within the Melilla Basin (Roger et al., 2000; Münch et al., 2001). The onset of diatomite formation of boreal affinity and the coeval development of a prograding bioclastic carbonate started around 6.73 ± 0.02 Ma, while a change from boreal to warm floral assemblages, marking the onset of the carbonate reef complex, is dated at 6.46 ± 0.01 Ma. The progradation of the carbonate reef complex, displayed by *Porites*-reef build-ups and the production of *Halimeda*-algae beds, ended prior to 6.0 ± 0.1 Ma. This final phase of open marine deposition was precluded by the end of diatomite deposition, dated at 6.29 ± 0.02 Ma (Roger et al., 2000; Münch et al., 2001).

3. Sections and lithostratigraphy

This paper concentrates on three Neogene marl sections in the Melilla Basin: namely, the Izarorene section located west of the Gourougou volcanic complex, and the Messâdit and Ifounassene sections exposed along the west and east coast of the Cap de Trois Fourges peninsula (Fig. 1). The sections are characterized by well-developed bipartite, and in part tripartite, sedimentary cycles, which consist of sub-horizontally bedded, laminated diatomaceous marls



Izarorene



Stratigraphic level (m)

10
0

alternating with homogeneous (sandy) marls. The nature of the sedimentary cycles closely resembles those observed in other astronomically calibrated Upper Miocene Mediterranean sequences.

3.1. The Izarorene section (IZ)

Approximately 5 km west of the Gourougou volcano, several marl-cliffs with a height of 80 m outcrop over a Quaternary plain near the Kert river, forming the sections of Samar (SA-1 section of Cunningham et al., 1997) and Izarorene (Fig. 1; Arias et al., 1976). The lower part of the Izarorene section is composed of a 50 m thick dark blue, poorly stratified, homogeneous clayey marl overlying a 2-m-thick, white ash (Fig. 2; 7^{bis-ter} of Arias et al., 1976; IR-1.0 of Cunningham et al., 1997). The distinct upward transition from the homogeneous clays to a pronounced, six-fold bipartite marl–diatomite alternation marks the onset of sedimentary cyclicity in the top part of the section (Fig. 2, Event A). These six cycles are numbered upward in stratigraphical order (IZc1 to IZc6) and consist of 1–3 m thick, finely laminated diatomites, and 3–6 m thick homogeneous marls, which grade from brownish gray to bluish marine deposits, and include a variety of macrofauna, e.g. abundant echinoids and crabs. Within the homogeneous marls of IZc3 several tephra layers are present, corresponding to the 11^{bis}–14^{ter} ashes of Arias et al. (1976). In addition, two thin volcano-clastic layers are located at the base of IZc5 and within the marl IZc6, respectively. Unconformably overlying the cyclic succession is a reddish clay covered by a sandstone.

3.2. The Messâdit section (ME)

The Messâdit section is located along the western coast of the peninsula, in the hillside opposite the village of Messâdit (Fig. 1; Gaudant et al., 1994; Saint Martin and Cornée, 1996; Rachid et al., 1997). It consists of a 70 m thick, well-exposed, blue-to-brownish diatomaceous marl sequence, rich in ostracods and bivalves. Several volcanic tuffs and ashes are intercalated, corresponding to tephrae dated by Roger et al. (2000) and Münch et al. (2001). The Neogene sequence

comprises a total of 35 well-defined, mostly bipartite sedimentary cycles capped by a *Halimeda*-algae packstone. These cycles are numbered successively with increasing stratigraphic level, hereafter referred to as MEC1 to MEC35 (Fig. 2).

The base of the section is formed by a volcanic tuff. An angular unconformity separates this ash from the underlying glauconitic sand unit, described by several authors as a “Basal Messinian glauconitic conglomerate above the Tortonian substratum” (e.g. Gaudant et al., 1994; Rachid et al., 1997). The tuff is directly overlain by a blue clayey marl, followed by twelve bipartite cycles composed of indurated cherty laminites and homogeneous sediments (MEC1–MEC12). These basal cycles have an average thickness of 200 cm, except for MEC7 (380 cm) and MEC11 (370 cm). The first of these cycles (MEC1) marks the onset of sedimentary cyclicity in this section (Event A). Additionally, a conspicuous change in color from bluish to brownish-gray marls is observed in MEC6 (Event B in Fig. 2).

The base of MEC13 marks the next distinct change in lithology from cherty laminites to well-developed white diatomites (indicated as Event C in Fig. 2). Numerous sponge spicules, bivalve fragments, bryozoans, planktonic and benthic foraminifera and abundant fish remains are found from this level upwards. Additionally, MEC15 to MEC20 display a change to tripartite cyclicity, in which the diatomites grade upward into reddish-brown laminated marls, followed by grayish homogeneous silty marls containing numerous oysters. From MEC21 upward, bipartite sedimentary cyclicity of distinct diatomites and homogeneous brown marls is continued. The laminite of MEC21 is thin (22 cm) compared to other laminites (30–50 cm). MEC24 contains an extreme thick diatomite bed (213 cm), above which two levels rich in *Neopycnodonte* oysters are recorded. This oyster-rich level can be traced along the entire outcropping cliff.

The sedimentary cyclicity is less regularly developed from MEC29 upward, due to an increase in siliciclastic influx. Nevertheless, a variety of bipartite lithological alternations is observed. Both MEC29 and MEC33 are composed of thin, pronounced diatomites and brown, homogeneous silty marls. MEC32 and MEC34 consist of

Fig. 2. Lithostratigraphic columns of the sampled sections in the Melilla Basin. The biostratigraphic marker events registered within the sections are: 1) FCO *G. nicolae* at 6.829 Ma, 2) LO *G. nicolae* at 6.712 Ma, 3) FCO *G. obesa* at 6.611 Ma, 4) *N. acostaensis* at 6.336–6.358 Ma (Krijgsman et al., 1999a; Sierro et al., 2001, converted to La2004), and 5) 1st sinistral influx of the *N. acostaensis* at 6.124 Ma. Numbers A–E denote the biostratigraphic events recorded within the Melilla Basin: A) onset of sedimentary cyclicity and diatomite deposition, B) lithology transition, C) onset of pronounced diatomite blooms associated with tropical-water conditions, D) final diatomite deposition, and E) onset of *Halimeda*-algae units covering the basinal sequences. On the right-hand side of the stratigraphic columns, the sedimentary-cycle numbers are included. The numbering on the left-hand side indicates volcanic and volcano-clastic levels.

thick, cherty diatomites, while MEc30 contains a vaguely laminated diatomaceous marl. Within MEc31, a bipartite alternation of a gray indurated marl and a soft brown marl is taken as a possible extra bipartite interval (MEc31a). The uppermost interval of the section (above laminite MEc34) consists of an alternation of silty marl, gray indurated marl and soft brownish marl, most likely representing the last bipartite couples (MEc35) prior to the deposition of the capping *Halimeda*-algae packstone.

A total of 19 tephras intercalated in the cyclic marls have been found and partly sampled for isotopic dating (Fig. 2). The stratigraphic position of the tephras forms an additional correlation tool and especially allows the Messâdit section to be correlated to the Ifounassene section (Table 2; Roger et al., 2000; Münch et al., 2001).

3.3. The Ifounassene section (IF)

The Ifounassene section is formed by a steep-sided coastal cliff incised by two narrow river valleys just north of the border with the Spanish enclave of Melilla and corresponds to the basal part of the Rostrogordo section (Saint Martin and Rouchy, 1986; Cunningham et al., 1994; Gaudant et al., 1994; Rachid et al., 1997). The section is composed of a cyclic marl sequence with a stratigraphic thickness of 30 m. It is capped by a pronounced *Halimeda*-algae packstone, which can be traced land-inwards towards the prograding reef complex (Cunningham et al., 1994). A total of 17 bipartite sedimentary cycles are recorded, consisting of an alternation of laminated lithologies and homogeneous, partly silty marls, which have been numbered in a stratigraphic order from base to top (named as IFc1–IFc17, Fig. 2). The laminated lithologies grade from clayey laminites to well-developed (cherty) diatomites, containing abundant bryozoan and bivalve fragments as well as shallow benthic foraminifera. By contrast, planktonic foraminifera are more dominant in the homogeneous sandy marls, where bryozoans are usually less abundant.

The base of the section is formed by a volcanic tuff (Ifo-1/2), which covers gray, homogeneous marls with load-structures. This tuff is overlain by two laminated, dark-brown clays, which grade upward into homogeneous clay (IFc1–IFc2). The interval above the basal clay is characterized by a diatomaceous sequence, comprising nine cycles of which the individual cycle thickness varies significantly (range: 170–230 cm). An extreme thick diatomite (230 cm) characterizes IFc5, above which two distinct *Neopycnodonte* levels occur within a homogeneous marl, as in MEc24. Within the

homogeneous interval of IFc7, mixing with volcanoclastic detritus occurs. A thin diatomaceous cycle (27 cm), including a concentrated ash layer (Ifo-4 ash) is present above this level. Cycles IFc12 to IFc15 consist of a bipartite cyclicity of laminated, partly diatomaceous marls alternating with silty homogeneous marls, which are in general burrowed and contain abundant mollusks, sponge spicules and a variety of shallow marine macro-fauna (fish, echinoids). The uppermost part of the section is composed of an alternation of homogeneous, fine-grained yellow sands, two laminated thin cherts (IFc15a and IFc17) and a diatomaceous, laminated marl (IFc16). These layers are covered by the *Halimeda* algae packstone, which contains thin silt intercalations as well as a thin, well-developed volcanic ash (most likely V3 of Cunningham et al., 1994 and Mes-19, Ifo-6, this study).

4. Biostratigraphy

The planktonic foraminiferal biostratigraphy of the Melilla Basin is based on the stratigraphic distribution of selected marker species, which occur synchronously over the Mediterranean basin and have been astronomically dated (Krijgsman et al., 1999a; Sierro et al., 2001). Five marker events have been identified in the Melilla Basin (Figs. 2 and 4, Table 1). Ages of astronomically dated bio-events are converted to the La2004_(1,1,0) solution.

The basal sediments of the Izarorene and Messâdit sections contain forms of the *Globorotalia miotumida*

Table 1
Biostratigraphic marker events recorded within the Melilla Basin

Event	Bio-sedimentary events	ATS age (Ma)
A	Onset (cyclic) diatomite deposition	6.84
1	FO <i>G. nicolae</i>	6.829
B	Color change from bluish to brownish grey marls	6.72
2	LCO <i>G. nicolae</i>	6.712
3	FaO <i>G. obesa</i>	6.611
C	Onset tropical diatomite blooms	6.58
–	Monospecific <i>G. bulloides</i>	6.47–6.43
–	<i>G. quinquiloba</i> and <i>G. multiloba</i> (peak on transition UA15-UA16 in Sorbas)	6.41–6.39
4	Sinistral/Dextral coiling change <i>N. acostaensis</i>	6.358–6.336
5	Sinistral influx <i>N. acostaensis</i>	6.124
D	Final diatomite bloom	6.11
E	Base of <i>Halimeda</i> -bed	6.08

The astronomical ages correspond to ATS ages of Krijgsman et al. (1999a) and Sierro et al. (2001) converted to La2004. Ages of events A–E are astronomically tuned ages in the Melilla Basin.

group, indicating that both sections were deposited above the first common occurrence of the group of *G. miotumida*, astronomically dated at 7.238 Ma (Hilgen et al., 1995; Sierro et al., 2001). This event can be used as a reliable marker of the Tortonian–Messinian boundary since it closely coincides with its global boundary stratotype recently defined in Morocco at 7.246 Ma (Hilgen et al., 2000a,b).

In the lowermost part of Messâdit and Izarorene, the first occurrence (FO) of the *Globorotalia nicolae* was observed below the second cherty indurated level, while its last common occurrence (LCO) is located above the sixth diatomite in Izarorene and right below diatomite MEC7 in Messâdit. The FO of *G. nicolae* was first identified and astronomically dated (6.829 Ma) in the Faneromeni and Metochia sections in Greece (Hilgen et al., 1995; Krijgsman et al., 1995). Both the FO and the LCO of the species were also recognized in the Abad composite section in SE Spain that has been proposed as the reference section for the Late Messinian part of the ATS (Sierro et al., 2001). They were astronomically dated at 6.829 and 6.712 Ma, respectively.

Intermediate specimens between *Globigerina obesa* and *Globigerinella siphonifera* are relatively rare in Izarorene and the lower part of the Messâdit section, but a prominent incursion of these forms was identified in the brownish marls above indurated layer MEC11. The FCO of these forms are also observed in the Abad composite section and other Mediterranean sections (6.611 Ma; Sierro et al., 2001, 2003).

A prominent sinistral-to-dextral coiling change of *Neogloboquadrina acostaensis* is located slightly above the extremely thick diatomites in the Messâdit and Ifounassene sections (MEC24/IFc5). A similar change has been recorded in the pre-evaporite marls of many Mediterranean sections and in the North Atlantic, slightly predating the onset of the latest Miocene glaciation (Hodell et al., 1989, 1994, Krijgsman et al., 1999a; Hilgen and Krijgsman, 1999; Sierro et al., 2001; Hodell et al., 2001; Krijgsman et al., 2002). It is therefore astronomically dated at 6.358 Ma. Above this event, the Neogloboquadrinids are dominantly dextral coiled, but a prominent influx of sinistral forms was identified within the homogeneous marls of cycle MEC33 and IFc15. This bio-event was correlated with the first of two influxes of sinistral Neogloboquadrinids occurring in Spain, Italy and Greece below the onset of the evaporite deposition (Hilgen and Krijgsman, 1999; Krijgsman et al., 1999a; Sierro et al., 2001) and dated at 6.124 Ma. The uppermost levels of Messâdit and Ifounassene are almost devoid of planktonic foraminif-

era, preventing the recognition of other younger foraminiferal events in this part of the sections.

Additionally, the common to abundant occurrence of *Turborotalita quinqueloba* and *Turborotalita multiloba* in cycle MEC22, and the abundant, almost monospecific, occurrence of *Globigerina bulloides* in cycles MEC18 and MEC19 in Messâdit, can be used as secondary bio-events (Table 1). Similar events have been observed in the Abad composite section in SE Spain from 6.47 to 6.43 Ma (Sierro et al., 2001, 2003).

5. Magnetostratigraphy

Oriented samples have been taken from each section for paleomagnetic analysis at a resolution of at least 5 drilled levels per sedimentary cycle, using an electrical field-drill and magnetic compass. To avoid overprinting by weathering, samples (2.5 cm diameter each) were taken from material as fresh as possible. A total of 222 sample-levels were drilled: 30 at Izarorene, 141 at Messâdit and 51 at Ifounassene. Paleomagnetic analysis in the laboratory included stepwise (per 30 °C) thermal demagnetization and measurement of NRM decay was performed on a 2G DC SQUID cryogenic magnetometer. Tectonic correction was not necessary because of sub-horizontal bedding of the sections.

The bulk of the samples typically display a weak magnetic signal (<1 mA/m). Generally, a two-component magnetization is observed, consisting mostly of a sub-recent normal overprint (80–210 °C) and a characteristic remanent magnetization (ChRM). This ChRM could be isolated after moderate thermal demagnetization (240–390 °C). Stepwise demagnetization was continued until complete removal of the high-temperature component or until the NRM became inconsistent or scattered.

Several demagnetization diagrams are given in Fig. 3, showing examples of samples with either a clear polarity (Fig. 3A,B), a valid but extremely weak signal (Fig. 3C), or a clustering at temperatures ranging from 200 to 480 °C (Fig. 3D). Other samples show poorly or unreliably determined components, as the NRMs bypass the origin, after which a clustering is observed (Fig. 3E), or consist only of scattering (Fig. 3F). The latter types of samples do not yield any reliable results regarding polarity. Therefore, the polarity zones as shown in Fig. 4, are based on the first group of data.

The magnetostratigraphic results of Izarorene display a reversed polarity interval for the lower part of the section, whereas no reliable results are available for the

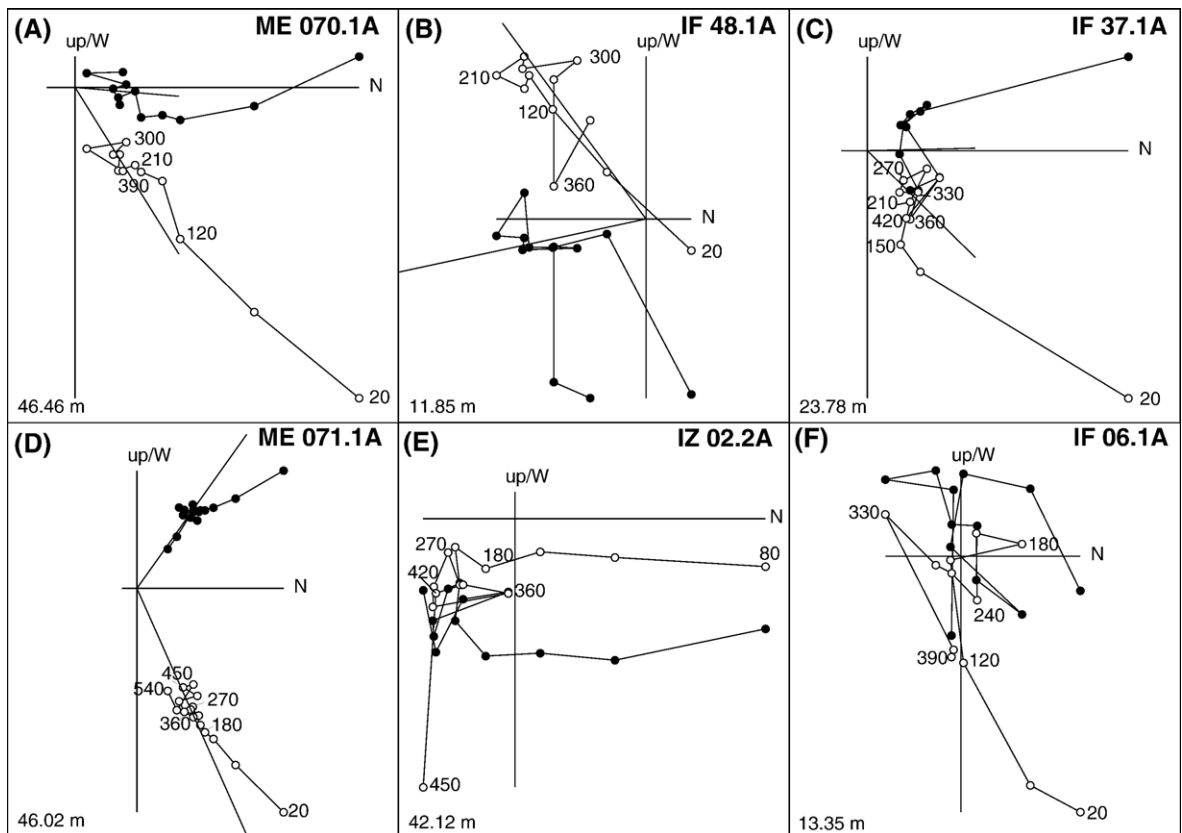


Fig. 3. Stepwise thermal demagnetization (Zijderveld) diagrams of selected samples from the Izarorene, Messâdit, and Ifounassene sections. Closed (open) symbols denote the projection of the ChRM vector end-points on the horizontal (vertical) plane. The included values represent temperature in °C; stratigraphic levels are included in the lower left corners.

top of the section. The basal 15 m of Messâdit do not display a clear polarity, whereas a N–R–N polarity is apparent for the main part of the section. Between MEC5 and MEC19, the section shows an overall normal polarity, followed by a reversed interval between MEC20 and MEC27, changing into a normal polarity from MEC27 upwards. The basal 10 m of the Ifounassene section have not been sampled for magnetostratigraphy. From IFc6 to IFc10 the section is reversed, whereas from IFc11 upward the section displays normal polarity.

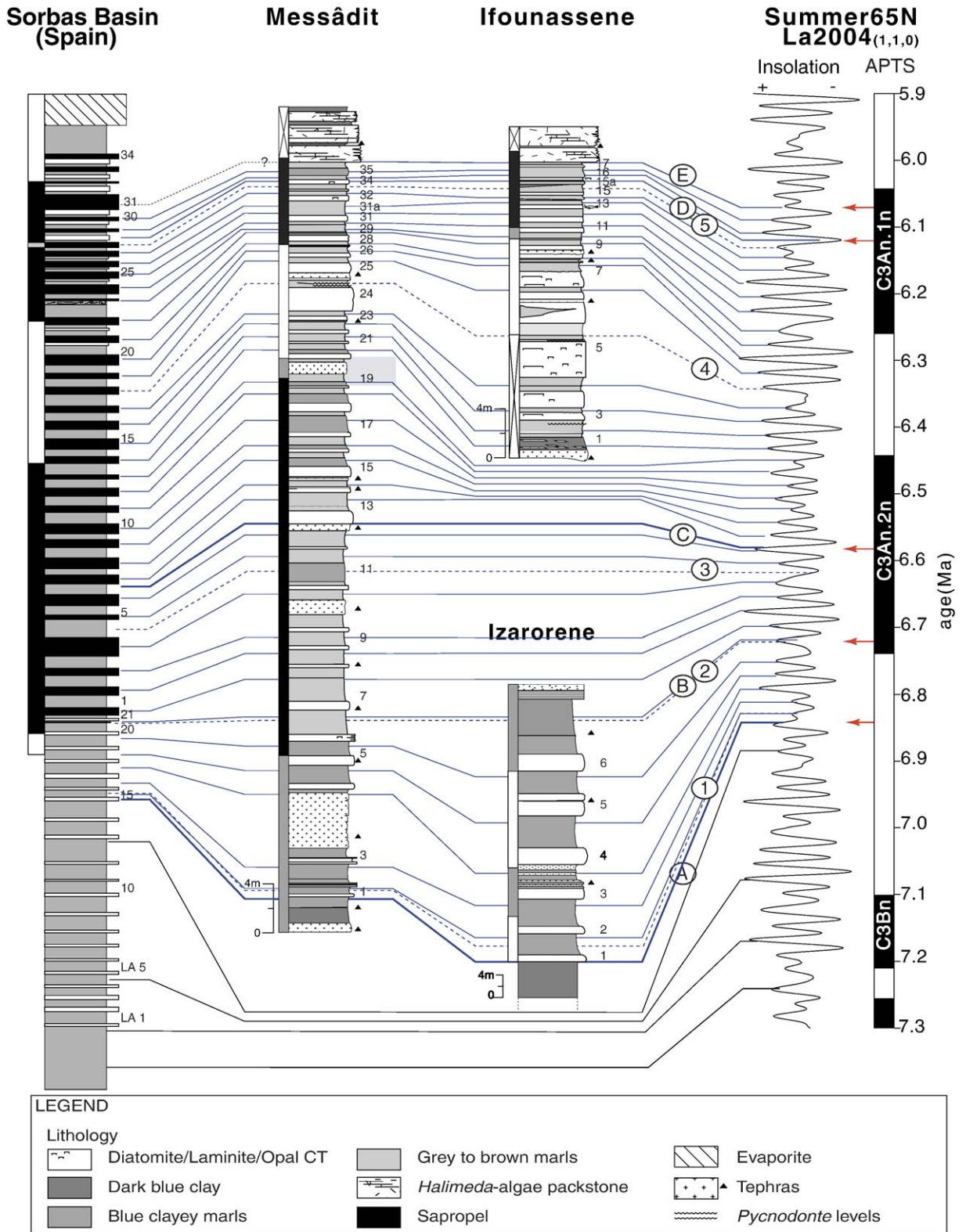
We can conclude that the paleomagnetic signal of the Melilla Basin displays a weak but straightforward

R–N–R–N reversal pattern, although no certainty can be given on the precise location of each reversal.

6. Integrated stratigraphic framework

The astronomical tuning of the Neogene marl sequence of the Melilla Basin is primarily based on the recognition of planktonic foraminiferal events. A large number of late Neogene bio-events are synchronous over the Mediterranean Basin, as demonstrated by detailed biostratigraphic studies on astronomically calibrated Mediterranean sections (Hilgen et al., 1995; Hilgen and Krijgsman, 1999; Sierro et al., 2001). Five of

Fig. 4. High-resolution astrochronological tuning of the basinal sections of the Melilla Basin. The tuning is based on the biostratigraphic position of astronomically calibrated marker events (Events 1–5), in comparison to the sedimentary cyclicity (lithostratigraphic columns). The magnetostratigraphic columns (included on the left side of each lithostratigraphic column) enable further comparison to the APTS curve at the right. Black (white) intervals represent normal (reversed) polarity, the polarity in the gray intervals is uncertain. The composite section of the Sorbas basin in southern Spain is included for comparison to other astrochronologically-tuned sequences in the Mediterranean basin. Based on a repetitive pattern of abundant planktonic foraminifera within the homogeneous marl intervals and numerous bryozoa fragments, echinoids, fish fragments etc. and only sparse planktonic foraminifera within the laminated intervals, astronomical tuning of the sedimentary cyclicity is based on the relationship that the top of the homogeneous levels corresponds to insolation maxima. This is equivalent to a similar pattern in Sorbas.



these have been identified in the Melilla Basin. The stratigraphic order of these events, supplemented by the ATS ages, is (Figs. 2 and 4; Krijgsman et al., 1999a):

- 1) FO of *G. nicolae* at 6.829 Ma,
- 2) LCO of *G. nicolae* at 6.712 Ma,
- 3) FAO of *G. obesa* at 6.611 Ma,
- 4) Sinistral-to-dextral coiling change of *N. acostaensis* at 6.358–6.336 Ma,
- 5) First sinistral influx of *N. acostaensis* at 6.124 Ma.

The accurate age-control of these planktonic foraminiferal events allows direct correlation of the bipartite sedimentary cycles to the summer insolation target-curve of Laskar (La2004_(1,1,0); Laskar et al., 2004; Fig. 4). The phase-relation of the sedimentary cyclicity with respect to the target curve is primarily based on the lithostratigraphic position of the tuned bio-events, supplemented by variations in planktonic foraminiferal assemblage and abundance per lithology. Overall, the homogeneous intervals contain a high planktonic foraminiferal content and minor amounts of bryozoan and bivalve fragments within the homogeneous intervals, while a reduction in planktonic foraminifera and large amounts of mainly bryozoans are observed within the laminated lithologies. This alternation resembles a similar pattern in the Upper Abad member of the Sorbas Basin (Sierro et al., 2001, 2003), in which a strong periodic reduction in the abundance of planktonic foraminifera occurs near the transition from homogeneous marls to sapropels. Moreover, the presence of warm-oligotrophic foraminifera within the upper part of the homogeneous marls of several cycles in the Melilla Basin corresponds to a similar pattern within the sapropels of the Upper Abad. Based on these repetitive patterns, we suggest a bed-to-bed correlation of the upper part of the homogeneous marls in Melilla to the sapropels in Sorbas. Since sapropels are undoubtedly linked to precession minima and insolation maxima, we therefore assume that the homogeneous levels in Melilla correlate to the summer insolation maxima.

The stratigraphic position of the biomarker events from the FO of *G. nicolae* (6.829 Ma) to the *N. acostaensis* coiling change (6.358–6.336 Ma), and the number of cycles between these marker events within the Melilla Basin, are similar to astronomically calibrated Mediterranean sections. Moreover, characteristic patterns in the target curve are mirrored by the more-than-average cycle thickness of MEc11 and MEc24/IFc5: the extra thick marl of MEc11 corresponds to a precession cycle with a prolonged period of 29 kyr, correlating to the cycle UA4 in Sorbas, and

the thick diatomite of MEc24/IFc5 corresponds to a double minimum peak at 6.358–6.336 Ma (Fig. 4; Krijgsman et al., 1999a; Sierro et al., 2001). The resulting astronomical tuning of the sections indicates that no cycles are missing in this interval of the sedimentary record, and moreover confirms the precession-induced origin of the sedimentary cycles of the Melilla Basin (Fig. 4). The tuning has resulted in astronomical ages for the bio-sedimentary events of the Melilla Basin: 6.84 Ma for the onset of diatomaceous cyclicity (Event A), 6.72 Ma for the marl-lithology and faunal transition (Event B), and 6.58 Ma for the start of pure diatomite deposition in the basin (Event C).

Tuning of the interval above the *N. acostaensis* coiling change is less straightforward due to an increased terrigenous influx and enhanced volcanic activity. In particular, the lithology alternations at Messâdit are, in part, poorly developed. At Ifounassene, however, a total of ten sedimentary repetitions are present between the *N. acostaensis* coiling change datum and the first sinistral influx level of the *N. acostaensis* (6.124 Ma), which is in perfect agreement with ten sedimentary cycles in the Sorbas basin and the ten insolation minimum peaks in the ATS (Fig. 4). We therefore change to the Ifounassene section for the upward continuation of the astronomical calibration, making use of the *Pycnodonte* level located above the coiling change level in both sections. As a result, the youngest diatomite bed in the basin (2 m below the *Halimeda*-algae packstone) has an astronomical age of 6.11 Ma (Event D in MEc34/IFc16). Because another two sedimentary cycles are present above this youngest diatomite both at Ifounassene and Messâdit, the onset of the *Halimeda*-packstone has an astronomical age of 6.08 Ma (Event E).

The tuning of the individual sedimentary cycles of the Melilla Basin to the ATS also provides astronomical ages for the intercalated ashes. These are given in Table 2, in which they are compared with the isotopic ⁴⁰Ar/³⁹Ar ages of Cunningham et al. (1994, 1997) and Roger et al. (2000).

Even though part of the paleomagnetic signal of the sampled marls is unreliable, the magnetostratigraphic results are in good agreement with the presented biostratigraphy (Fig. 4). Our results are consistent with the findings of Cunningham et al. (1994, 1997), and show that the normal polarity intervals correspond to the chrons C3An.1n and C3An.2n (Cande and Kent, 1995). Several minor discrepancies, however, do occur between the APTS and the cyclostratigraphic position of the reversals in the Melilla Basin. The C3An.2n(y) reversal is recorded in the homogeneous marl of MEc19,

Table 2

Compilation of astronomical and isotopic ($^{40}\text{Ar}/^{39}\text{Ar}$) ages of the volcanic ashes embedded in the Messinian marls and carbonate sequences of the Melilla Basin

Section	ATS age (Ma)	Isotopic age (Ma)
<i>Izarorene</i>		
Iza-3	6.730	-
Iza-2	6.760	-
Iza-1	6.794	11 ^{bis} -14 ^{ter} : 5.6±0.3 (K/Ar biotite) ^a 5.9±0.3 (K/Ar biotite) ^a 7.1±0.4 (K/Ar biotite) ^a 6.7±0.6 (FT glass) ^a 6.6±1.0 (FT glass) ^a
Basal cinerite	>6.84	IR-1.0: 6.90±0.02 ^b 7 ^{bis-ter} : 6.8±0.3 (K/Ar glass) 6.0±0.3 (K/Ar glass) ^a 6.4±0.6 (FT glass) ^a 6.3±0.6 (FT glass) ^a 6.8±1.2 (FT glass) ^a
<i>Messâdit</i>		
Mes-19	6.05±0.02	V3: 6.0±0.1 ^b
Mes-18	6.259	-
Mes-17	6.298	Located ^c
Mes-16	6.312	-
Mes-15	6.336	-
Mes-14	6.378	-
Mes-13	6.386	-
Mes-12	6.452	-
Mes-11	6.542	Located ^c
Mes-10	6.552	-
Mes-9	6.581	Me16: 6.46±0.03 ^c
Mes-8	6.638	Me13: 6.54±0.04 ^c
Mes-7	6.687	-
Mes-6	6.716	-
Mes-5	6.762	-
Mes-4	6.791	V2: 6.72±0.02 ^b V2: 6.76±0.02 ^b Me5: 6.73±0.02 ^c
Mes-1	>6.84	Located ^c
<i>Ifounassene</i>		
Ifo-6	6.05±0.02	V3: 6.0±0.1 ^b If-4: 6.29±0.02 ^c
Ifo-5	6.269	-
Ifo-4	6.280	-
Ifo-3	6.325	-
Ifo-2	6.442	-
Ifo-1	6.452	-

The ashes are ordered by their stratigraphic position. The astronomical ages are obtained by a bed-to-bed correlation of the marl sections to the ATS (Krijgsman et al., 1999a; Sierro et al., 2001). The isotopic ages of Cunningham et al. (1997) have been recalculated relative to FCT of 28.02 Ma (Renne et al., 1998). The located ashes of Roger et al. (2000), represent ashes which are mentioned in the article of Roger et al. (2000) without $^{40}\text{Ar}/^{39}\text{Ar}$ dates. 1 σ analytical error is displayed. FT = fission track ages.

^a Arias et al. (1976).

^b Cunningham et al. (1997).

^c Roger et al. (2000).

which is one cycle below its ATS position. This shift can be attributed to a delayed acquisition of the magnetic signal, which is a commonly observed phenomenon in cyclically bedded sequences of the Mediterranean Neogene (Van Hoof and Langereis, 1992). Again, a similar discrepancy is observed for C3An.1n(o) in Messâdit (MEc27), whereas the recording of this reversal in Ifounassene is at least two sedimentary cycles higher in the stratigraphic sequence with respect to Messâdit (Fig. 4).

7. Discussion

7.1. Comparison to previous work on the Melilla Basin

Previous geochronological studies in the Melilla Basin mainly concerned isotope geochronology and were focused on the petrology and volcanology of the domes and lava flows of the Gourougou and Trois Fourches volcanic complexes (e.g. Hernandez and Bellon, 1985; Cunningham et al., 1994, 1997; El Bakkali et al., 1998; Roger et al., 2000). Münch et al. (2001) and Cornée et al. (2002) focus on the geochronology and development of the carbonate platform and its basinal equivalents using $^{40}\text{Ar}/^{39}\text{Ar}$ ages of volcanic horizons. Several of the volcanic horizons described in these studies are located in the astronomically tuned sections of this study. Astronomical ages can therefore be assigned to $^{40}\text{Ar}/^{39}\text{Ar}$ dated volcanic tephtras and the results of two independent dating methods can be compared (Table 2). The $^{40}\text{Ar}/^{39}\text{Ar}$ ages of Cunningham et al. (1994, 1997), have been recalculated with the Fish Canyon Tuff standard (FCT) of 28.02 Ma (Renne et al., 1998) to allow a reliable comparison of different studies.

Cunningham et al. (1997) have dated the basal ash in the Izarorene section at 6.90±0.02 Ma (Table 2). This isotopic age is in good agreement with our findings, because the first astronomically dated sedimentary cycle (IZc1), dated at 6.85 Ma, is located 40 m above this ash layer (IR-1 ash in Table 2; Cunningham et al., 1997). The tephtras between sedimentary cycles IZc3 and IZc4, corresponding to the 11^{bis}-14^{ter} ashes of Arias et al. (1976), have an astronomical age of 6.79 Ma, which falls within the 2 σ error of the isotopic ages of ~6.7 Ma (FT age). Nevertheless, we prefer not to take into account the K/Ar and fission track (FT) ages of the latter study in the comparison of astronomical and isotopic ages, because of their low accuracy and precision.

Roger et al. (2000) studied six volcanic horizons interbedded in the Messâdit section from which three have been used for $^{40}\text{Ar}/^{39}\text{Ar}$ dating. The most

straightforward correlation of these volcanic horizons to the ash layers found in our study is given in Table 2. Based on their stratigraphic position within the Messâdit section, the following correlation can be given. The three most pronounced volcanic ashes in Messâdit are the thick ash (Mes-4) in the lower part, and the Mes-8 and Mes-9 ashes in the central part of the section. These ashes correspond respectively to the Me-5, Me-13 and Me-16 ashes of Roger et al. (2000).

Cunningham et al. (1994, 1997) sampled and dated two volcanic tuffs (V1 and V2 in their Irhzer Ifzatene section) in the bioclastic platform north of Ifounassene. These two ashes are likely the equivalents of the lowermost ashes of our study (Mes-1 and Mes-4). Similar to our Mes-1 ash, V1 is located directly above glauconitic ramp deposits at the base of the marl sequence, while V2 is located 10 m above V1 within the lowermost marls at a comparable position as our Mes-4. V2 therefore has a younger isotopic age of ~6.74 Ma with respect to the inferred ATS age of 6.79 Ma (Table 2), whereas V1 is clearly older than the onset of sedimentary cyclicity within the basin. Comparison of the isotopic and astronomical ages of these ashes indicates that the $^{40}\text{Ar}/^{39}\text{Ar}$ ages in Messâdit are systematically younger than the astronomical counterparts (Table 2).

$^{40}\text{Ar}/^{39}\text{Ar}$ ages are also available for several volcanic layers in the Ifounassene section (Cunningham et al., 1997; Roger et al., 2000; Münch et al., 2001). Although stratigraphic distances in the Rostrogrado section of Münch et al. (2001) do not fully agree with ours, their three volcano-clastic horizons most likely correspond with our Ifo-3, Ifo-4 and Ifo-5 ashes (Fig. 2). Roger et al. (2000) have only dated one volcanic tuff (If-4) below the *Halimeda*-index bed, but the stratigraphic position of this ash is uncertain. Based on the correlation of their work to that of Münch et al. (2001), the If-4 ash of Roger et al. (2000) might be the lateral equivalent of our Ifo-5 ash (Table 2). This is mainly supported by the ash thickness, which implies, however, that the $^{40}\text{Ar}/^{39}\text{Ar}$ age of this volcanic tuff is slightly older than its stratigraphic position would suggest (Table 2).

Additionally, Cunningham et al. (1997) sampled ash V3 above the *Halimeda*-index bed. Because the base of this *Halimeda*-bed forms the top of the astronomically tuned part of our section, V3 must be younger than the ATS age of 6.05 Ma (Fig. 4), which is in agreement with the isotopic age (6.0 ± 0.1 Ma in Table 2; Cunningham et al., 1997).

In summary, the $^{40}\text{Ar}/^{39}\text{Ar}$ ages of three tephtras in Messâdit are systematically younger than the astronomical ages of these layers, while at Ifounassene the correlation is not certain. As previously mentioned, all

$^{40}\text{Ar}/^{39}\text{Ar}$ ages have been calculated with the currently common-used age of 28.02 Ma for the Fish Canyon Tuff sanidine mineral dating standard of Renne et al. (1998). A recent discussion about the precision and accuracy of the absolute ages of neutron fluence monitors and decay constants used in $^{40}\text{Ar}/^{39}\text{Ar}$ geochronology (Begemann et al., 2001) calls for new assessment of these parameters. A shift towards slightly older absolute ages for the Fish Canyon Tuff, based on U/Pb dating on zircon and titanite (Schmitz and Bowring, 2001) will result in older absolute $^{40}\text{Ar}/^{39}\text{Ar}$ ages reducing the age differences between the isotopic and astronomical ages in Messâdit. Roger et al. (2000) assign $^{40}\text{Ar}/^{39}\text{Ar}$ ages to three main pre-evaporitic bio-sedimentary events within the Melilla Basin, for which we have now derived the astronomical ages (Events A, C and E). The differences between the astronomical and isotopic ages of these events resulted in part from the differences in dating method, as described above. An additional error stems from the lack of a stratigraphic correction in the study of Roger et al. (2000), who simply assign the $^{40}\text{Ar}/^{39}\text{Ar}$ age of the tephra nearest to a biostratigraphic event to this event, without correcting for the time between the event and the deposition of the tephra.

7.2. Comparison to the pre-evaporitic Messinian

The integrated stratigraphic framework of this study provides high-resolution dating of the open marine marls of the Melilla Basin. Comparison of these results to both Rifian and Mediterranean basins emphasizes the role of the Melilla Basin in the evolution of the Rifian Corridor. Although no details can yet be given on the onset of marine sedimentation within the Melilla Basin itself, the occurrence of Messinian homogeneous marine clays overlying “Tortonian” glauconitic sands, implies a rapid transgression prior to 6.84 Ma at which moment open marine, cyclic sedimentation started (Event A). Several authors argue an early Messinian age for the basal blue, homogeneous clayey marls, in which case these deposits are coeval with the “late Tortonian–early Messinian Blue Marls” in the Taza–Guercif, Saïss and Chelif basins in the Rifian Corridor (Bernini et al., 1992; Krijgsman et al., 1999a; Mansour and Saint Martin, 1999; Barbieri and Ori, 2000; Gelati et al., 2000). The late Tortonian deepening of these central Rifian basins is attributed to an advancing thrust front in the central part of the Rif (Sani et al., 2000), corresponding to the Late Miocene compression within the Alboran Basin (e.g. Comas et al., 1992; Sani et al., 2000). Rapid uplift of these basins resulted after 7.17 Ma in the obstruction of Atlantic water inflow and therefore the onset of closure

of the Rifian Corridor (Krijgsman et al., 1999b). This early Messinian restriction of marine water-exchange through the Rifian Corridor is thought to have caused a so-called siphoning of cold Atlantic waters into the western Mediterranean (e.g. Benson et al., 1991; Cunningham and Collins, 2002). This might explain the cold-water signature within the first open marine deposits in the Melilla Basin (Fig. 5; Barbieri et al., 1976; Benmoussa et al., 1987).

At 6.84 Ma (Event A), cyclic sedimentation was triggered within the deeper parts of the Melilla Basin, while in the nearshore zone surrounding the Trois Fourges and Gourougou volcanoes, carbonate ramp deposition was replaced by a prograding bioclastic

platform (unit 2 of Saint Martin and Cornée, 1996; Roger et al., 2000). Saint Martin and Cornée (1996) attribute this depositional change to a transgressive to highstand relative sea-level fluctuation, coincident with an increased influx of boreal prone-waters (Rachid et al., 1997). Our astronomical tuning allows the testing of this hypothesis by a high-resolution correlation to the climate $\delta^{18}\text{O}$ record of the world oceans (Fig. 5; Hodell et al., 1994; Hodell et al., 2001). It then appears that the onset of cyclicality within the Melilla Basin does not correspond to a significant decrease in $\delta^{18}\text{O}$ of the world ocean (Fig. 5; Hodell et al., 2001). Since no coeval, evident depositional changes have been recorded for other Mediterranean basins at 6.85 Ma, a

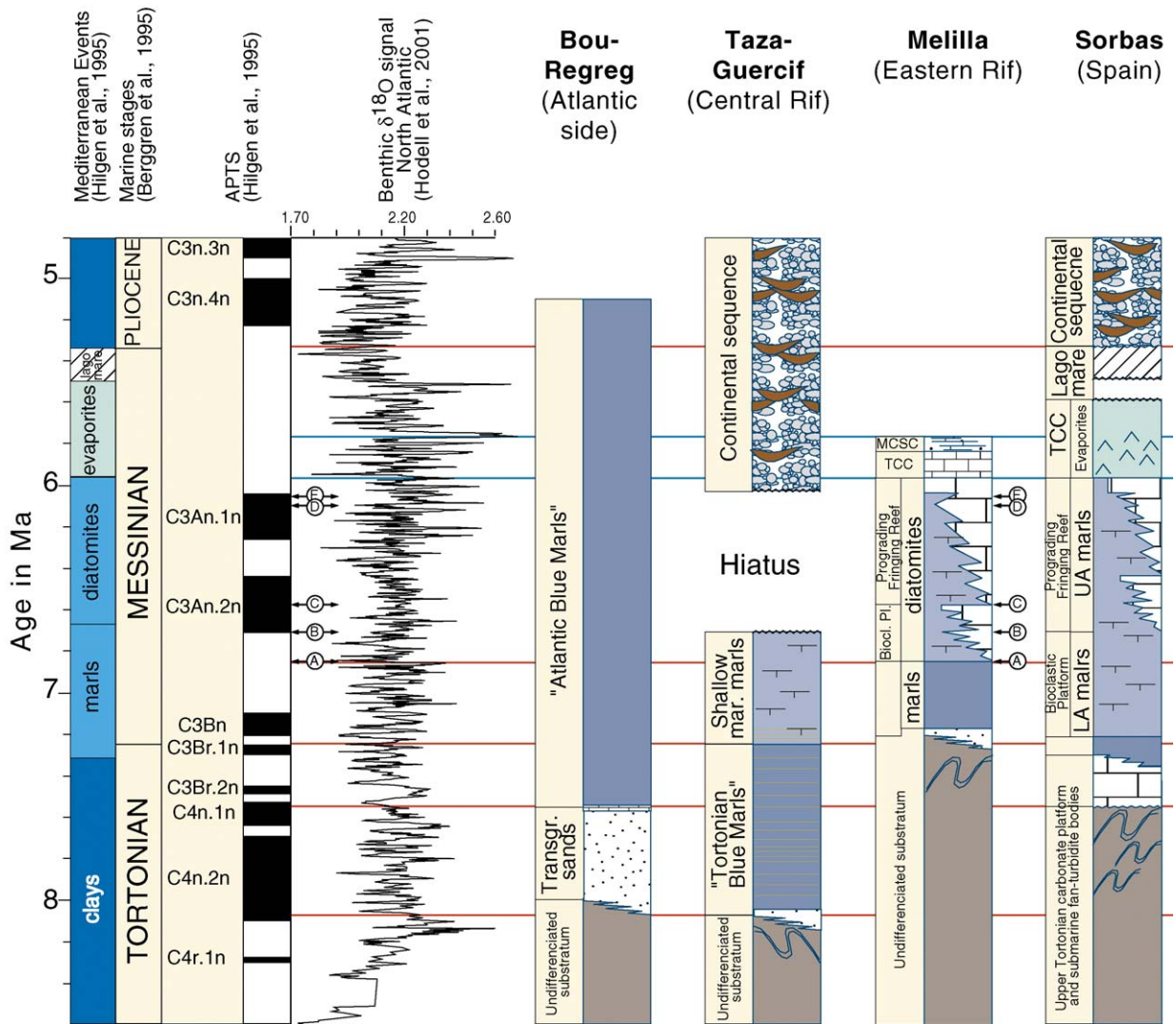


Fig. 5. Regional correlation between major basin components of the Rifian Corridor for the Late Miocene. Time-calibration is based on the astronomical tuning of various sections in each of the basins, including the Melilla Basin. MCS and TCC stand for the brackish to continental Mixed Carbonate Siliciclastic Complex and Terminal Carbonate Complex, respectively.

climate-induced sea-level rise can therefore not be considered as the triggering mechanism for Event A (Figs. 4 and 5). Moreover, the possibility of enhanced influx of boreal-prone waters through the Rifian Corridor is not supported by the shallow marine facies in the Taza–Guercif Basin (Fig. 5; Krijgsman et al., 1999b; Gomez et al., 2000). Tectonic activity within the Rif is therefore the most likely triggering mechanism for the change in depositional environment within the Melilla Basin at 6.84 Ma.

The distinct lithology transition of Event B above the *G. nicolae* Zone (6.72 Ma; Figs. 2 and 4) is recorded both within the Izarorene and Messâdit sections. Event B marks the prominent coeval change in the benthic foraminiferal assemblages that flourish in restricted waters. This suggests a sudden restriction of bottom water circulation at 6.72 Ma, which resulted in lower rates of oxygen turnover in the Melilla Basin. Final marine deposition upon the western plain of the Melilla Basin is halted directly above Event B (e.g. Izarorene section), which coincides with the base of the unconformity marking the nearshore-continental transition in the Taza–Guercif Basin (Krijgsman et al., 1999b).

Coeval to Event B is the lower-to-upper-Abad transition in the Sorbas Basin in Spain (Figs. 4 and 5), which is generally attributed to an increase in tectonic activity in the internal Betics (Fig. 5; Martín and Braga, 1994; Sierro et al., 2001, 2003). A coeval increase in tectonic activity is present within the Rif.

The transition from indurated cherty layers to white, mm-laminated diatomites in Messâdit is indicated as Event C (MEc13; 6.58 Ma) and corresponds to the change from boreal-prone to tropical diatom assemblages within the marginal facies (Saint Martin and Rouchy, 1986; Saint Martin and Cornée, 1996; Cunningham and Collins, 2002). Roger et al. (2000) correlate this transition to the onset of prograding *Porites*-fringing reefs of the carbonate platform (unit 3 of Cunningham et al., 1994; Saint Martin and Cornée, 1996). This is supported by the presence of abundant influx of bryozoan-fragments starting at the base of diatomite of MEc13 (Event C). Although several authors attribute this (bio-) facies transition to an increased nutrient supply caused by enhanced upwelling (Saint Martin and Cornée, 1996; Rachid et al., 1997; Pestrea et al., 1999; Roger et al., 2000), we infer that increased upwelling rates are not supported by either observations from the central Rifian basins, or by the fact that temperate water-conditions were replaced by (sub-) tropical conditions (Gaudant et al., 1994). Cunningham and Collins (2002), on the other hand, have suggested that this transition marks the end of an early Messinian siphoning of

Atlantic waters through the Rifian Corridor. This would explain both the transition in benthic taxa in the marginal facies as well as the transition from temperate-type limestone facies (molechfor) to (sub-) tropical limestone facies (chlorozoan) on the carbonate platform (Cunningham and Collins, 2002).

The youngest diatomites recorded in the basin have an astronomical age of 6.11 Ma (Event D). This latest diatomite bloom (Roger et al., 2000) marks the end of a continuous period of 730 kyr of cyclic diatomite deposition, the last 460 kyr of which are represented by pronounced diatomites (MEc13 to MEc34/IFc15a). The stratigraphic interval between this last diatomite bloom and the base of the *Halimeda*-packstone contains one or two precession-induced lithology cycles. Hence, we propose an astronomical age of at most 6.08 Ma for the base of the *Halimeda*-packstone and therefore for the final open marine deposition within the Melilla Basin (Event E). Since Münch et al. (2001) and Roger et al. (2000) indicate that the *Halimeda*-packstones form the basinal equivalent of the *Porites*-reefs in the Melilla Basin, we can now confirm their conclusion that the progradation of the *Porites* reefs ended prior to 6.0 Ma. Comparison of our work to the extensive work done on the carbonate platform of the Melilla Basin (Roger et al., 2000) implies that the aggrading *Porites* reefs (Fringing Reef unit of Cunningham et al., 1994, 1997) developed prior to the onset of Mediterranean evaporites (120 kyr before its start at 5.96 Ma; Krijgsman et al., 1999a, 2001, 2002). In addition, the onset of the Terminal Carbonate Complex (TCC — sensu Esteban, 1979) draping the carbonate platform can be considered coeval to the onset of the Lower Evaporites within the Mediterranean (Cunningham et al., 1994, 1997; Krijgsman et al., 2001; Fortuin and Krijgsman, 2003).

Additionally, the final open marine deposition within the Melilla Basin, as indicated by Event E, and the following final *Porites* reef progradation is roughly coeval with the emergence of the Taza–Guercif Basin (Krijgsman et al., 1999b). Altogether, these results imply a closure of the Rifian Corridor prior to 6.0 Ma, which is also suggested by the earliest African-European mammal-migration, dated roughly at 6.1 Ma (Benammi et al., 1996; Garcés et al., 1998).

8. Conclusions

Based on a detailed study of the Messinian marine marl sequence of the Melilla Basin, we can present a high-resolution time frame for this basin, with main emphasis on the importance of timing with respect to the evolution of the Rifian Corridor. Five bio-sedimentary

marker events, representing time horizons for the Messinian evolution of the Mediterranean Realm, have been recorded within the studied basinal marl sequence. These marker events confirm a bed-to-bed correlation between the studied sections, which is based on the recognition of a cyclic pattern in lithology. We achieved a direct correlation of our sections to astronomically tuned sequences within the Mediterranean Sea and the insolation curve of Laskar (La2004_(1,1,0); Laskar et al., 2004), showing a precession-dependence of the sedimentary cyclicity in the Melilla Basin.

The resulting astronomical time frame significantly refines the timing for three basin-evolution events presented in previous articles by the French (Saint Martin and co-workers), and exemplifies the importance of the Melilla Basin with respect to the evolution of the Rifian Corridor. The new astrochronology for the marl sequences of the Melilla Basin allows an accurate dating of the stepwise restriction of the Mediterranean–Atlantic connection through Morocco, including the following events:

- The onset of marine sedimentation within the Melilla Basin coincides with a tectonically induced shallowing of the Taza–Guercif Basin, and possibly with the onset of siphoning of Atlantic intermediate water through the narrowing Rifian Corridor. This phase appears moreover to be coeval to the deepening of several Betic Corridor basins (e.g. Sorbas and Nijar).
- The initiation of cyclic deposition (Event A) in the Melilla Basin started at 6.84 Ma. This event marks a restriction in paleo-circulation within the basin, and was reflected by the onset of the progradation of a bioclastic platform along shore.
- The bio-lithofacies transition of Event B at 6.72 Ma, coincides with main events within the Mediterranean, including the lower–upper Abad transition in Sorbas, and is coeval with the erosion-controlled closure or even emergence of the Taza–Guercif area.
- Event C marks at 6.58 Ma the onset of white diatomite deposition reflecting a change in diatom species from boreal-to-tropical species and is coincident with the onset of prograding *Porites* reefs along the platform. We believe therefore that this event most likely reflects a decrease in upwelling rates and thus diminishing input of cold Atlantic waters (end of siphoning of Benson et al., 1991).
- Closure of the open marine realm of the Melilla Basin was indicated by the final diatomite bloom (Event D at 6.11 Ma), followed by the production of *Halimeda*-algal beds, covering the cyclic marl sequence, starting at 6.08 Ma (Event E).

In summary, we conclude that the onset of open marine deposition within the Melilla Basin was initiated by tectonic activity of the Rif. The refined timing clearly shows that input of Atlantic waters through the Rifian Corridor was restricted after 6.84 Ma, and reduced to a minimum at 6.58 Ma. Moreover, the end of open marine deposition prior to 6.0 Ma supports the theories of a Terminal Carbonate Complex (TCC) as the marginal equivalent of the evaporites of the Messinian Salinity Crisis. The high-resolution timing of the Melilla Basin indicates that the importance of diatomite sequences of the ‘Tripoli’-type within Mediterranean basins reflects a superposition of local basin-configurations upon changes in the Mediterranean-wide paleo-circulation. Finally, the comparison of the isotopic ages for the bio-sedimentary basin-events (Cunningham et al., 1997; Roger et al., 2000; Münch et al., 2001) to our new astronomically calibrated ages indicates that the isotopic ages are dominantly younger.

Acknowledgements

We acknowledge P. Renne and A. Deino with whom we shared fieldwork. We are very grateful to C.G. Langereis and F.J. Hilgen for their critical comments and to S. Iaccarino and M. Garcés for their constructive reviews of the manuscript. This study forms part of the research program of the Vening Meinesz Research School of Geodynamics (VMSG) and the Netherlands Research School of Sedimentary Geology (NSG) and is financially supported by the Netherlands Research Centre for Integrated Solid Earth Science (ISES). The project was furthermore supported by an ALW grant to K.F. Kuiper, while F.J. Sierro was supported by the MCYT project BTE2002-04670.

References

- Arias, C., Bigazzi, G., Bonadona, F.P., Morlotti, E., di Brozolo, F. R., Rio, D., Torelli, L., Brigatti, M.F., Giuliani, O., Tirelli, G., 1976. Chronostratigraphy of the Izarôrene section in the Melilla basin (northeastern Morocco). *Boll. Soc. Geol. Ital.* 95, 1681–1694.
- Barbieri, R., Ori, G.G., 2000. Neogene palaeoenvironmental evolution in the Atlantic side of the Rifian Corridor (Morocco). *Palaeogeogr. Palaeoclimatol. Palaeoecol.* 163, 1–31.
- Barbieri, F., Morlotti, E., Palmieri, G., Rio, D., Torelli, L., 1976. Biostratigraphy of the Izarôrene section in the Melilla basin (NE Morocco). VII African Micropaleontological Colloquium ILE-IFE, Nigeria.
- Begemann, F., Ludwig, K.R., Lugmair, G.W., Min, K., Niquist, L.E., Patchett, P.J., Renne, P.R., Shih, C.Y., Villa, I.M., Walker, R.J., 2001. Call for an improved set of decay constants for geochronological use. *Geochim. Cosmochim. Acta* 65 (1), 111–121.

- Benammi, M., Calvo, M., Prévot, M., Jaeger, J.J., 1996. Magnetostratigraphy and paleontology of Ait Kandoula basin (High Atlas, Morocco) and the African–European Late Miocene terrestrial fauna exchanges. *Earth Planet. Sci. Lett.* 145, 15–29.
- Benmoussa, A., Demarcq, G., Lauriat-Rage, A., 1987. Pectinides messiniens du Bassin de Melilla (NE Maroc); comparaisons inter-regionales et intérêts paleobiologiques. *Rev. Paleobiol.* 6 (1), 111–129.
- Benson, R.H., Rakic-El Bied, K., Bonaduce, C., 1991. An important reversal (influx) in the Rifian Corridor (Morocco) at the Tortonian–Messinian Boundary: the end of Tethys Ocean. *Paleoceanography* 6 (1), 164–192.
- Bernini, M., Boccaletti, M., El Mokhtari, J., Gelati, R., Iaccarino, S., Moratti, G., Papani, G., 1992. Données stratigraphiques nouvelle sur le Miocène supérieur du bassin de Taza–Guercif (Maroc nord-oriental). *J. Soc. Geol. Fr.* 163 (100), 73–76.
- Cande, S.C., Kent, D.V., 1995. Revised calibration of the geomagnetic polarity time scale for the late Cretaceous and Cenozoic. *J. Geophys. Res.* 100, 6093–6095.
- Choubert, G., Faure-Muret, A., Hottinger, L., Lecoindre, G., 1966. Le Néogène du bassin Melilla (Maroc septentrional) et sa signification pour définir la limite Mio–Pliocène au Maroc. *Comm. Médit. Neogene Strat. ICS-IUGS*, pp. 238–249.
- Comas, M.C., García-Dueñas, V., Jorado, M.J., 1992. Neogene tectonic evolution of the Alboran basin from MCS data. *Geo Mar. Lett.* 12, 157–164.
- Cornée, J.J., Saint Martin, J.P., Conesa, G., André, J.P., Müller, J., BenMoussa, A., 1996. Anatomie de quelques plates-formes carbonatées progradantes messiniennes de Méditerranée occidentale. *Bull. Soc. Géol. Fr.* 167 (4), 495–507.
- Cornée, J.J., Roger, S., Münch, P., Saint Martin, J.P., Féraud, G., Conesa, G., Pestrea, S., 2002. Messinian events: new constraints from sedimentological investigations and new $^{40}\text{Ar}/^{39}\text{Ar}$ ages in the Melilla–Nador basin (Morocco). *Sediment. Geol.* 151, 127–147.
- Cunningham, K.J., Collins, L.S., 2002. Control on facies and sequence stratigraphy of an upper Miocene carbonate ramp and platform, Melilla basin, NE Morocco. *Sediment. Geol.* 146, 285–304.
- Cunningham, K.J., Farr, M.R., Rakic-El Bied, K., 1994. Magnetostratigraphic dating of an Upper Miocene shallow-marine and continental sedimentary succession in northeastern Morocco. *Earth Planet. Sci. Lett.* 127, 77–93.
- Cunningham, K.J., Benson, R.H., Rakic-El Bied, K., McKenna, L.W., 1997. Eustatic implications of late Miocene depositional sequences in the Melilla basin, northeastern Morocco. *Sediment. Geol.* 107, 147–165.
- El Bakkali, S., Bourdier, J.L., Gourgaud, A., 1998. Caractérisation et stratigraphie de dépôts volcanoclastiques marqués dans le Miocène supérieur de bassin de Melilla-bas Kert (Rif oriental, Maroc). *C.R. Acad. Sci. Paris* 327, 93–100.
- Esteban, M., 1979. Significance of the Upper-Miocene coral reefs of the western Mediterranean. *Palaeogeogr. Palaeoclimatol. Palaeoecol.* 29, 169–188.
- Fortuin, A.R., Krijgsman, W., 2003. The Messinian of the Nijar basin (SE Spain): sedimentation, depositional environments and paleogeographic evolution. *Sediment. Geol.* 160, 213–242.
- Garcés, M., Krijgsman, W., Agustí, J., 1998. Chronology of the Late Turolian deposits of the Fortuna basin (SE Spain): implications for the Messinian evolution of the eastern Betics. *Earth. Planet. Sci. Lett.* 163, 69–81.
- Gaudant, J., Saint Martin, J.P., BenMoussa, A., Cornée, J.J., El Hajjaji, K., Müller, J., 1994. L'ichthyofaune messinienne à la périphérie de la plate-forme carbonatée de Melilla–Nador (nord-est du Maroc). *Géol. Méd.* 21 (1–2), 25–35.
- Gelati, R., Giovanna, M., Papani, G., 2000. The Late Cenozoic sedimentary succession of the Taza–Guercif Basin, South Rifian Corridor, Morocco. *Mar. Petrol. Geol.* 17 (3), 373–390.
- Gomez, F., Barazangi, M., Demnati, A., 2000. Structure and evolution of the Neogene Guercif Basin at the junction of the Middle Atlas Mountains and the Rif Thrust Belt, Morocco. *AAPG Bull.* 84 (9), 1340–1364.
- Guillemin, M., Houzay, J.P., 1982. Le néogène post–nappe et le Quaternaire de Rif nord-oriental (Maroc): Stratigraphie et tectonique des bassins de Melilla, du Kert et du piedmont des Kebbana. *Notes Mém. Serv. Géol. Maroc* 314, 7–238.
- Hernandez, J., Bellon, H., 1985. Chronologie K–Ar du volcanisme Miocène du Rif oriental (Maroc): implications tectonique et magmatiques. *Rev. Géol. Dyn. Géogr. Phys.* 26 (2), 85–94.
- Hilgen, F.J., Krijgsman, W., 1999. Cyclostratigraphy and astrochronology of the Tripoli diatomite formation (pre-evaporite Messinian, Sicily, Italy). *Terra Nova* 11, 18–22.
- Hilgen, F.J., Krijgsman, W., Langereis, C.G., Lourens, L.J., Santarelli, A., Zachariasse, W.J., 1995. Extending the astronomical (polarity) time scale into the Miocene. *Earth Planet. Sci. Lett.* 136, 495–510.
- Hilgen, F.J., Bissoli, L., Iaccarino, S., Krijgsman, W., Meijer, R., Negri, A., Villa, G., 2000a. Integrated stratigraphy and astrochronology of the Messinian GSSP at Oued Akrech (Atlantic Morocco). *Earth Planet. Sci. Lett.* 182, 237–251.
- Hilgen, F.J., Iaccarino, S., Krijgsman, W., Langereis, C.G., Villa, G., Zachariasse, W.J., 2000b. The Global Boundary Stratotype Section and Point (GSSP) of the Messinian Stage (uppermost Miocene). *Episodes* 23, 172–178.
- Hodell, D.A., Benson, R.H., Kennett, J.P., Rakic-El Bied, K., 1989. Stable isotope stratigraphy of late Miocene–early Pliocene sequences in Northwest Morocco: the Bou Regreg section. *Paleoceanography* 4 (4), 467–482.
- Hodell, D.A., Benson, R.H., Kent, D.V., Boersma, A., Rakic-El Bied, K., 1994. Magnetostratigraphic, biostratigraphic, and stable isotope stratigraphy of an upper Miocene drill core from Salé Briqueterie (Northwestern Morocco). A high resolution chronology for the Messinian stage. *Paleoceanography* 9, 835–855.
- Hodell, D.A., Curtis, J., Sierro, F.J., Raymo, M., 2001. Correlation of late Miocene-to-early Pliocene sequences between the Mediterranean and North Atlantic. *Paleoceanography* 16 (2), 164–179.
- Krijgsman, W., Hilgen, F.J., Langereis, C.G., Santarelli, A., Zachariasse, W.J., 1995. Late Miocene magnetostratigraphy, biostratigraphy and cyclostratigraphy in the Mediterranean. *Earth Planet. Sci. Lett.* 136, 475–494.
- Krijgsman, W., Hilgen, F.J., Raffi, I., Sierro, F.J., Wilson, D.S., 1999a. Chronology, causes and progression of the Messinian Salinity Crisis. *Nature* 400, 652–655.
- Krijgsman, W., Langereis, C.G., Zachariasse, W.J., Boccaletti, M., Moratti, G., Gelati, R., Iaccarino, S., Papani, G., Villa, G., 1999b. Late Neogene evolution of the Taza–Guercif Basin (Rifian Corridor, Morocco) and implications for the Messinian Salinity Crisis. *Mar. Geol.* 153, 147–160.
- Krijgsman, W., Fortuin, A.R., Hilgen, F.J., Sierro, F.J., 2001. Astrochronology for the Messinian Sorbas Basin (SE Spain) and orbital (precessional) forcing for evaporite cyclicity. *Sediment. Geol.* 140, 43–60.
- Krijgsman, W., Blanc-Valleron, M.M., Flecker, R., Hilgen, F.J., Kouwenhoven, T.J., Merle, D., Orszag-Sperber, F., Rouchy, J.-M., 2002. The onset of the Messinian salinity crisis in the Eastern Mediterranean (Pissouri Basin, Cyprus). *Earth Planet. Sci. Lett.* 194, 299–310.

- Laskar, L.J., Robutel, P., Joutel, F., Gastineau, M., Correia, A.C.M., Levrard, B., 2004. A long term numerical solution for the insolation quantities of the Earth. *Astron. Astrophys.* 428, 261–285.
- Mansour, B., Saint Martin, J.P., 1999. Conditions de dépôt des diatomites messiniennes en contexte de plate-forme carbonatée d'après l'étude des assemblages de diatomées: exemple du Djebel Murdjadjo (Algérie). *Geobios* 32 (3), 395–408.
- Martín, J.M., Braga, J.C., 1994. Messinian events in the Sorbas Basin in southeastern Spain and their implications in the recent history of the Mediterranean. *Sediment. Geol.* 90, 257–268.
- Münch, P., Roger, S., Cornée, J.J., Saint Martin, J.P., Féraud, G., BenMoussa, A., 2001. Restriction des communications entre l'Atlantique et la Méditerranée au Messinien: apport de la téphrochronologie dans la plate-forme carbonatée et le bassin de Melilla–Nador (Rif nord-oriental, Maroc). *C.R. Acad. Sci. Paris* 332, 569–576.
- Pestrea, S., Mansour, B., Saint Martin, J.P., 1999. Diatomites du Messinien d'Afrique du Nord (Algérie, Maroc): Principaux enseignements. *Cryptogam., Algol.* 20, 109–110.
- Rachid, A., El Hajjaji, K., BenMoussa, A., 1997. Les associations foraminifères benthiques des séries marno–diatomitiques messiniennes du bassin de Nador–Melilla (Maroc nord oriental). *Géol. Méd.* 24 (1–2), 29–49.
- Renne, P.R., Swisher, C.C., Deino, A.L., Karner, D.B., Owens, T., De Paolo, D.J., 1998. Intercalibration of standards, absolute ages and uncertainties in $^{40}\text{Ar}/^{39}\text{Ar}$ dating. *Chem. Geol.* 145, 117–152.
- Roger, S., Münch, P., Cornée, J.J., Saint Martin, J.P., Féraud, G., Pestrea, S., Conesa, G., BenMoussa, A., 2000. $^{40}\text{Ar}/^{39}\text{Ar}$ dating of the pre-evaporitic Messinian marine sequences of the Melilla basin (Morocco): a proposal for some bio-sedimentary events as isochronous around the Alboran Sea. *Earth Planet. Sci. Lett.* 179, 101–113.
- Saint Martin, J.P., Cornée, J.J., 1996. The Messinian Reef Complex of Melilla, northeastern Rif, Morocco. *Soc. Econ. Paleontol. Mineral. Concepts Sedimentol. Paleontol. Ser.* 5, 227–238.
- Saint Martin, J.P., Rouchy, J.M., 1986. Intérêt du complexe récifal du Cap des Trois Fourges (Bassin de Nador, Maroc septentrional) pour l'interprétation paléogéographique des événements messiniens en Méditerranée occidentale. *C.R. Acad. Sci. Paris* 302, 957–962.
- Saint Martin, J.P., Cornée, J.J., Muller, J., Camoin, G., André, J.P., Rouchy, J.M., BenMoussa, A., 1991. Contrôles globaux et locaux dans l'édification d'une plate-forme carbonatée messinienne (bassin de Melilla, Maroc): apport de la stratigraphie séquentielle et de l'analyse tectonique. *C.R. Acad. Sci. Paris* 315, 1573–1579.
- Sani, F., Zizi, M., Bally, A.W., 2000. The Neogene–Quaternary evolution of the Guercif Basin (Morocco) reconstructed from seismic line interpretation. *Mar. Petrol. Geol.* 17, 343–357.
- Schmitz, M.D., Bowring, S.A., 2001. U–Pb zircon and titanite systematics of the Fish Canyon Tuff; an assessment of high-precision U–Pb geochronology and its application to young volcanic rocks. *Geochim. Cosmochim. Acta* 65 (1), 2571–2587.
- Sierro, F.J., Krijgsman, W., Hilgen, F.J., Flores, J.A., 2001. The Abad composite (SE Spain): Mediterranean reference section for the Messinian and the Astronomical Polarity Time Scale (APTS). *Palaeogeogr. Palaeoclimatol. Palaeoecol.* 168 (1–2), 143–172.
- Sierro, F.J., Flores, J.A., Francés, G., Vazquez, A., Utrilla, R., Zamarreño, I., Erlenkeuser, H., Barcena, M.A., 2003. Orbitally-controlled oscillations in planktic communities and cyclic changes in western Mediterranean hydrography during the Messinian. *Palaeogeogr. Palaeoclimatol. Palaeoecol.* 190, 289–316.
- Van Hoof, A.A.M., Langereis, C.G., 1992. The upper and lower Thvera sedimentary geomagnetic reversal records from southern Sicily. *Earth Planet. Sci. Lett.* 114, 59–76.